J. Mt. Sci. (2023) 20(2): 381-390 e-mail: jms@imde.ac.cn http://jms.imde.ac.cn
https://doi.org/10.1007/s11629-022-7691-0

Original Article

Spatial distribution and driving factors of sediment net nitrogen mineralization in riparian zone of the Three Gorges Reservoir

JIA Kai-tao[1] https://orcid.org/0000-0001-9274-7766; e-mail: 1580289098@qq.com

HE Li-ping[1*] https://orcid.org/0000-0001-9438-6175; e-mail: hlp_weird@163.com

WANG Ke-hong[1] https://orcid.org/0000-0001-9592-1221; e-mail: wang018837@hotmail.com

YU Zhi-guo[2] https://orcid.org/0000-0002-0909-6788; e-mail: zhiguo.yu@nuist.edu.cn

LIANG Li-jiao[1] https://orcid.org/0000-0003-1378-0993; e-mail: lianglijiao0326@163.com

YU Zhuo-lin[1] https://orcid.org/0000-0002-6061-2901; e-mail: yuchulin99@gmail.com

LIN Jun-jie[1*] https://orcid.org/0000-0003-0955-3106; e-mail: junjielin@sanxiau.edu.cn

**Corresponding author*

1 Key Laboratory of Water Environment Evolution and Pollution Control in the Three Gorges Reservoir, Chongqing Three Georges University, Chongqing 404100, China

2 School of Hydrology and Water Resources, Nanjing University of Information Science and Technology, Nanjing 210044, China

Citation: Jia KT, He LP, Wang KH, et al. (2023) Spatial distribution and driving factors of sediment net nitrogen mineralization in riparian zone of the Three Gorges Reservoir. Journal of Mountain Science 20(2). https://doi.org/10.1007/s11629-022-7691-0

Abstract: Inorganic nitrogen (N) loss through sediment N mineralization is important for eutrophication surrounding riparian zone. Sediment physicochemical properties have been changed at water-level elevation in riparian zone of the Three Gorges Reservoir (TGR) due to differences in hydrological stress and human activity intensity. However, spatial distribution and driving factor of net N mineralization rate (N_{min}) and its temperature sensitivity (Q_{10}) based on the changes in sediment physicochemical properties are still unclear at water-level elevation in the riparian zone. A total of 132 sediment samples in the riparian zone were collected including 11 transections and 12 water-level elevations on basin scale of the TGR during drying period, to conduct a 28-day incubation at 15°C, 22°C, 29°C and 36°C. N_{min}, total N (TN) and substrate quality (SQ) increased with water-level elevation, while Q_{10} showed an opposite trend (P<0.001). Results of the structural equation model showed that water-level elevation had direct positive effects on TN and SQ (P<0.01). In addition, TN was the major factor that had a direct positive effect on N_{min}, and SQ was the crucial factor that had a direct negative effect on Q_{10} (P<0.001). In conclusion, increases in TN and SQ were major driving factors of N_{min} and its Q_{10} at water-level elevation, respectively, in riparian zone of the TGR during drying period.

Keywords: Inorganic nitrogen loss; Sediment physicochemical properties; Drying period; Substrate quality; Net nitrogen mineralization rate; Temperature sensitivity

Received: 04-Sep-2022
Revised: 10-Oct-2022
Accepted: 17-Nov-2022

1 Introduction

Riparian zone is the transitional zone between land and aquatic ecosystems, which is important for quality of its surrounding water. Inorganic nitrogen (N) loss from riparian zone will migrate to its surrounding water, even leading to eutrophication (Wang et al. 2020; Zhao et al. 2021). Sediment net N mineralization is one of sources of inorganic N loss from riparian zone (Gilles et al. 2018; Lupon et al. 2016).

Driving factors of net N mineralization have been investigated under environments of drying, flooding and alternating drying and flooding in sediment of riparian zone. The results demonstrate that land use, topography, vegetation, revegetation and revetment are driving factors of net N mineralization rate (N_{min}) under the drying environment (Kikuchi et al. 2020; Yan et al. 2019; Ye et al. 2015; Zhang et al. 2021). Moreover, N_{min} is controlled by groundwater table under the flooding environment (Hefting et al. 2004). In addition, N_{min} is regulated by redox frequency change under environment of alternating drying and flooding (Zha et al. 2022). Recently, it was found that sediment physicochemical properties, such as sediment organic carbon (C, SOC), total N (TN) and C: N ratio, are inconsistent at different water-level elevations of riparian zone due to differences in hydrological stress and intensity of human activity (Li et al. 2020; Ran et al. 2020; Ye et al. 2020; Ye et al. 2019). However, spatial distribution of N_{min} and its driving factors based on changes of sediment physicochemical properties are still unclear at water-level elevation in riparian zone.

Except for the above driving factors, global warming is also responsible for the increase in N_{min} (Miller and Daniel 2018; Song et al. 2018). Temperature sensitivity (Q_{10}) of N_{min} represents response strength of sediment net N mineralization to the increase in temperature, which is important for assessing sediment N loss under background of global warming (Davidson and Janssens 2006; Kirschbaum 1995). Q_{10} varies widely among ecosystems, and differences in sediment properties are the main reason for this fluctuation (Liu et al. 2017). Among sediment properties, the difference in substrate quality (SQ) may be the major controlling factor for Q_{10} (Liu et al. 2016, 2017, 2020). Recalcitrant substrates with low SQ are more difficult to be decomposed by microorganisms than labile substrates with high SQ. According to the Arrhenius equation, the demand for activation energy (E_a) is higher for recalcitrant substrates than that for labile substrates during decomposition of organic substrates. Therefore, compared to labile substrates, the elevated temperature is more favorable to promoting mineralization of recalcitrant substrates (Craine et al. 2010; Fierer et al. 2005), which is known as the C quality temperature (CQT) hypothesis (Davidson and Janssens 2006; Fierer et al. 2005). In terms of soil N mineralization, this hypothesis has been confirmed in several ecosystems including forests, grasslands and farmlands (Liu et al. 2016, 2017, 2020). However, it is unclear what the Q_{10} is, whether the Q_{10} could be explained by CQT hypothesis, and what spatial distribution and driving factors of Q_{10} are in riparian zone.

Riparian zone of the Three Gorges Reservoir (TGR), with a total area of 349 km^2 (Bao et al. 2015), has undergone periodic drying and wetting cycles, resulting in significant loss of sediment N and changes in sediment properties after operation of the Three Gorges Dam, which threatens aquatic environment quality of the TGR (Yang et al. 2015). On the one hand, N in the sloping farmland is released to the TGR through interflow under runoff erosion (Wang et al. 2020), and spatial distribution of sediment N has been changed by hydrological stress (Ye et al. 2019). On the other hand, SOC, TN, pH (Ye et al. 2020; Ye et al. 2019; Shen et al. 2022), suspending solid deposition (Tang et al. 2018; Tang et al. 2016), particle-size distribution (Li et al. 2019) and aggregate size (Ran et al. 2020) have been changed by hydrological stress and human activities. However, the relationship between N loss and the changes in sediment physicochemical properties is unclear in the riparian zone at present. The answer to this problem could provide a scientific base for evaluating, preventing and controlling N release from riparian zone sediment to the TGR.

Since sediment TN decreases with submergence frequency (Li et al. 2020; Ye et al. 2020) and labile substrate input is higher at higher water-level elevation (Garssen et al. 2015; Ye et al. 2020), we hypothesized that N_{min} and its Q_{10} vary chiefly with sediment organic N content and SQ, respectively, at water-level elevation of the riparian zone. Objectives of this study are: (1) to investigate spatial distribution characteristics of N_{min} and its Q_{10} at water-level elevation of the riparian zone during drying period; (2) to reveal driving factors of N_{min} and its Q_{10} at

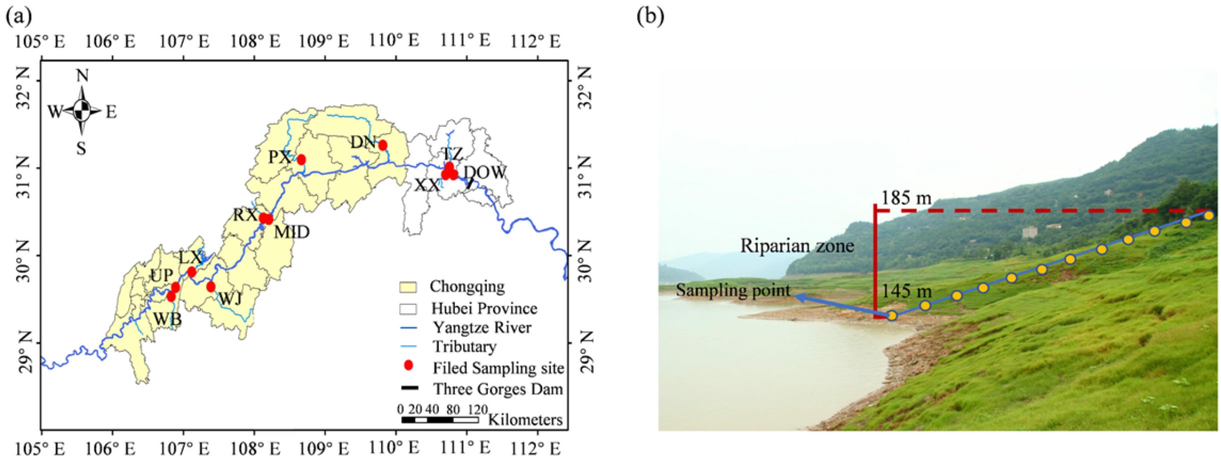

Fig. 1 Location of study sites (a) and distribution of sampling points on water-level elevations (b). UP, MID, and DOW are the upstream, midstream, downstream in the mainstream. Eight sample sites are WB (Wubu river), Longxi river (LX), Wujiang river (WJ), Ruxi river (RX), Pengxi river (PX), Daning river (DN), Xiangxi river (XX) and Tongzhuang river (TZ).

water-level elevation based on changes in sediment physicochemical properties and CQT hypothesis.

2 Materials and Methods

2.1 Site description and sampling

The TGR area is located upstream of the Yangtze River, stretching from Yichang city in Hubei Province to Jiangjin city in Chongqing. This area is characterized by a humid subtropical monsoon climate, with an average annual temperature of 16°C–19°C and average annual precipitation of 1000–1200 mm. For flooding control and power generation, water level of the TGR is artificially controlled, dropping from 175 m in January to 145 m in July and then gradually rising to 175 m in September. Flooding durations of water-level elevations of 145–155, 155–165 and 165–175 m are 263–363, 163–263 and 63–163 d $year^{-1}$, respectively (Chen et al. 2019). The riparian zone is usually exposed from April to September (drying period). Average daily temperature is 24.79 °C during the drying period, with minimum and maximum average daily temperatures of 15.56°C and 31.63°C, respectively. Regosols, Anthrosols and Luvisols are the chief soil types in this area (China soil database, http://vdb3.soil.csdb.cn). Regosols are developed from Trias-Cretaceous system of sedimentary rocks; Anthrosols are recognized by soils on which irrigated rice is chronically cultivated; Luvisols are derived from sand shale and the dominant clay mineral is vermiculite.

Three sample sites were selected including upstream (UP), midstream (MID) and downstream (DOW) in the mainstream (Fig. 1). In addition, eight sample sites were selected including Wubu river (WB), Longxi river (LX), Wujiang river (WJ), Ruxi river (RX), Pengxi river (PX), Daning river (DN), Xiangxi river (XX) and Tongzhuang river (TZ) in the tributaries. Twelve sediment samples were collected at each sample site of water-level elevations (Table 1). Finally, 132 sediment samples (0–20 cm) were collected via a sediment corer with a diameter of 5 cm in late July 2019. The sediment samples were stored in a vehicle-mounted refrigerator at 4°C and sent to the laboratory within 24 h. Each sample was freeze-dried, picked out of gravel, plant and animal debris, mixed evenly and divided into two subsamples. One of the subsamples was utilized for determination of sediment physicochemical properties including moisture content, sediment bulk density (SBD), pH,

Table 1 Information of the sampling sites

Sample sites*	Longitude	Latitude	Distance to TGD (km)
UP	106.88°E	29.62°N	420.94
MID	108.19°E	30.42°N	273.82
DOW	110.81°E	30.93°N	21.62
WB	106.84°E	29.57°N	426.13
LX	107.09°E	29.81°N	394.39
WJ	107.38°E	29.68°N	372.74
RX	108.14°E	30.40°N	279.16
PX	108.67°E	31.10°N	224.29
DN	109.82°E	31.28°N	123.81
XX	110.76°E	30.99°N	29.79
TZ	110.73°E	30.93°N	29.01

Note: Full names of the abbreviations for the sample sites can be found in Fig. 1.

TN, ammonium N (NH_4^+-N), nitrate N (NO_3^--N) and SOC (Appendix 1). The other subsamples were sieved through a 2 mm mesh for subsequent incubation.

2.2 Sediment incubation and analyses

Fifteen gram sediments for each sample, with three replicates, were evenly placed in 150 mL jars and incubated at temperatures of 15°C, 22°C, 29°C and 36°C. Incubation temperatures were designed with a gradient of 7°C in range of 15°C–36°C based on the minimum (15.56°C) and maximum (31.63°C) average daily temperatures during drying period. After adjusting sediment moisture to 60% of maximum water holding capacity using deionized water, the samples were incubated in dark for 28 days (N_{min} keeps stable at this time (Jia et al. 2019)). All samples were destructed and extracted with 0.5 M K_2SO_4 to determine sediment contents of NH_4^+-N and NO_3^--N at the end of the incubation.

Sediment pH was determined by a digital pH meter (1: 2.5 of sediment-water ratio). SBD and maximum water holding capacity were measured by the ring knife method and the gravimetric method, respectively. Sediment contents of NH_4^+-N and NO_3^--N were analyzed using the salicylate method (Verdouw et al. 1978) and the single reagent method (Doane and Horwáth 2003), respectively. SOC and TN were detected by an element analyzer (Nelson 1983, EA3000, Euro Vector, Milan, Italy).

2.3 Data analyses

Sediment net ammonification rate (N_{amm}), net nitrification rate (N_{nit}) and N_{min} (mg kg^{-1} d^{-1}) were calculated as follows (Eqs. 1-3, Liu et al. 2020):

$$N_{amm} = \frac{c(NH_4^+\text{-N})_{i+1} - c(NH_4^+\text{-N})_i}{\triangle t} \quad (1)$$

$$N_{nit} = \frac{c(NO_3^-\text{-N})_{i+1} - c(NO_3^-\text{-N})_i}{\triangle t} \quad (2)$$

$$N_{min} = N_{amm} + N_{nit} \quad (3)$$

where $c(NH_4^+\text{-N})_i$ and $c(NH_4^+\text{-N})_{i+1}$ are sediment contents of ammonium N before and after the incubation, respectively (mg kg^{-1}). $c(NO_3^-\text{-N})_i$ and $c(NO_3^-\text{-N})_{i+1}$ are sediment contents of nitrate N before and after the incubation, respectively (mg kg^{-1}). i and i+1 represent the initial and post incubation times, respectively. $\triangle t$ is the incubation time (days).

The reaction activation energy (E_a) was calculated by fitting N_{min} and T with the following equation (Eq. 4, Knorr et al. 2005):

$$N_{min} = A \times e^{\frac{-E_a}{RT}} \quad (4)$$

where N_{min} represents the net N mineralization rate (mg kg^{-1} d^{-1}); A is the frequency factor; E_a is the activation energy (kJ mol^{-1}); R is the gas constant (8.314 J mol^{-1} K^{-1}), and T is the incubation temperature (K).

We used Eq. 5 (Lloyd and Taylor 1994) to describe the relationship between N_{min} across the temperature range, and Q_{10} was calculated as Eq. 6 (Fierer et al. 2005; Liu et al. 2020):

$$N_{min} = SQ \times e^{kT} \quad (5)$$

$$Q_{10} = e^{10k} \quad (6)$$

where SQ is an exponential constant, which is an index of substrate quality, representing difficulty of microbial mineralization of nitrogen-containing organic substrates (Ding et al. 2016; Fierer et al. 2005). T is incubation temperature (K); k is temperature response coefficient.

Regression analyses were applied to explore relationships between SQ and E_a, Q_{10} and E_a, as well as water-level elevations and sediment physicochemical properties, SQ, N_{min} and its Q_{10}. Analysis of structural equation model showed multivariate effects of water-level elevation on N_{min} and its Q_{10} via pathways of sediment physicochemical properties. Fit of structural equation model was evaluated using the χ^2 test, the degree of freedom (df), the P-value, the root mean square error of approximation (RMSEA) and the comparative fit index (CFI). Data fittings were conducted by Origin 9.5 (Origin Lab Software Inc.). Structural equation model analysis was performed by IBM SPSS Amos 24 (IBM Corp., 2016).

3 Results

3.1 Sediment physicochemical properties

Sediment moisture content, SBD, TN and SOC ranged from 3.4% to 58.8%, 0.59 to 1.60 g cm^{-3}, 0.40 to 3.86 g kg^{-1} and 3.80 to 61.59 g kg^{-1}, respectively, at water-level elevations with medians of 26.06%, 1.24 g cm^{-3}, 1.22 g kg^{-1} and 15.88 g kg^{-1}, respectively (Fig. 2). TN and SOC increased linearly with water-level elevation (P<0.01), and sediment moisture, SBD and C: N ratio showed opposite trends (P<0.01).

3.2 Sediment N mineralization rates

N_{amm}, N_{nit} and N_{min} ranged from -1.98 to 3.49, -0.11 to 11.00 and -0.40 to 10.30 mg kg^{-1} d^{-1}, respectively, at water-level elevations, with medians of -0.28, 3.29 and 2.99 mg kg^{-1} d^{-1} (Fig. 3), respectively. N_{nit} and N_{min} increased linearly with water-level elevation at incubation temperatures (P<0.01), while no significant differences were observed for N_{amm} among water-level elevations (P>0.05).

3.3 Q_{10} of net N mineralization rate

Temperature sensitivity ranged from 0.59 to 4.84, with a median of 1.23, at water-level elevations (Fig. 4). A negative linear relationship was observed between Q_{10} and water-level elevations (P<0.001). SQ ranged from 0.01 to 8.29, with an average of 2.01. A positive linear relationship was detected between SQ and water-level elevations (P<0.001). Q_{10} increased exponentially with E_a (Fig. 5, R^2=0.95, P<0.001); instead, E_a declined exponentially with SQ (R^2=0.56, P<0.001). As a low SQ value (low-quality organic compounds) means substrate is difficult to be decomposed by microorganisms, the results indicated that low-quality organic compounds with high E_a exhibited a higher proportional increase in N_{min} compared to higher-quality organic compounds when incubation temperature increased, which is consistent with the CQT hypothesis.

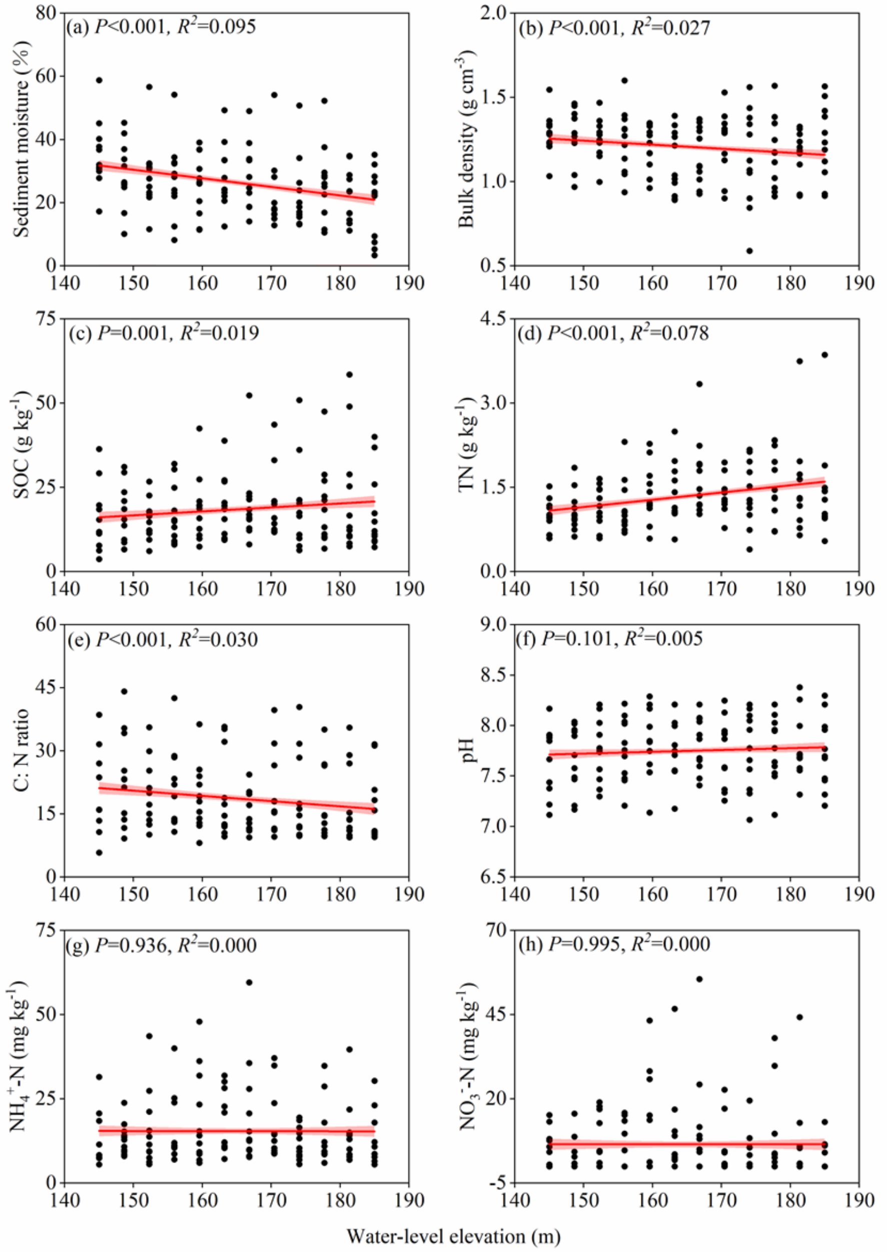

Fig. 2 Relationships between sediment physicochemical properties and water-level elevations (n=132). Solid red lines represent fitted lines, and red areas below solid red lines are 95% confidence intervals. Subfigures a, b, c, d, e, f, g and h show changes in sediment moisture, bulk density, sediment organic carbon (SOC) content, total N content, C: N ratio, pH, ammonium and nitrate concentration, respectively, at water-level elevations.

3.4 Driving factors of N_{min} and Q_{10}

Water-level elevation had a direct negative effect on sediment moisture and SBD (Fig. 6, P<0.001), a direct positive effect on SOC, TN and SQ (P<0.01), and a further indirect positive effect on N_{min} through TN and SOC (P<0.01). Water-level elevation had an indirect positive effect on Q_{10} through SBD and TN, and an indirect negative effect on Q_{10} through SQ (P<0.001).

4 Discussion

Our results indicated that N_{min} increased with water-level elevation, while its Q_{10} showed an opposite trend. Moreover, N_{min} and its Q_{10} were primarily controlled by raise of TN and SQ with water-level elevation, respectively, which is consistent with our hypothesis. The results would be helpful for evaluation, prevention and control of sediment N release from the riparian zone to its surrounding water and deepen our understanding of key processes of sediment net N mineralization in the riparian zone.

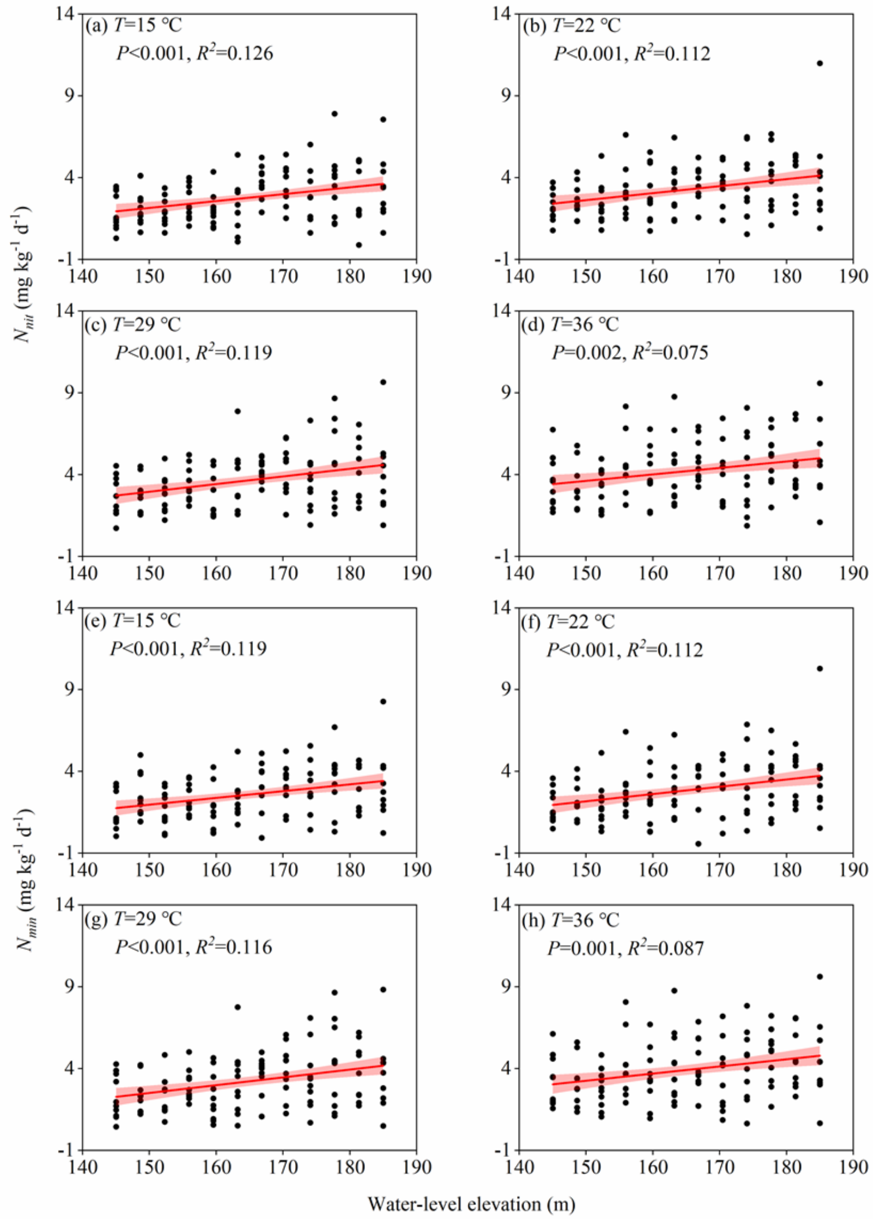

Fig. 3 Relationships between net nitrification rate (N_{nit})/net N mineralization rate (N_{min}) and water-level elevations in the riparian zone (n=132). Solid red lines represent fitted lines, and red areas below solid red lines are 95% confidence intervals. (a), (b), (c), and (d) show changes in N_{nit}, and (e), (f), (g), and (h) show changes in N_{min} at 15°C, 22°C, 29°C and 36 °C, respectively.

4.1 Sediment N mineralization rates

Soil net N mineralization rate increased with water-level elevation (Fig. 3, P<0.05). Raise of TN with water-level elevation (Fig. 2) was responsible for the result due to higher vegetation biomass at high water-level elevations compared to low water-level elevations in riparian zone of the TGR (Garssen et al. 2015; Ye et al. 2020), supported by results of the structural equation model (Fig. 6). An *in situ* study demonstrated that N_{min} is mainly controlled by groundwater table in riparian zone (Hefting et al. 2004). Meanwhile, an incubation experiment showed that N_{min} is chiefly controlled by fluctuation of oxidation-reduction potential caused by alternation sediment environment of drying and flooding in riparian zone (Zha et al. 2022). Both these reported results are inconsistent with our results. The reasons for these discrepancies are differences in sediment environment. In our study, we discussed N_{min} under drying environment rather than under environments of flooding and alternation drying and flooding. Thus, further studies should be conducted to investigate spatial distribution and driving factors of N_{min}

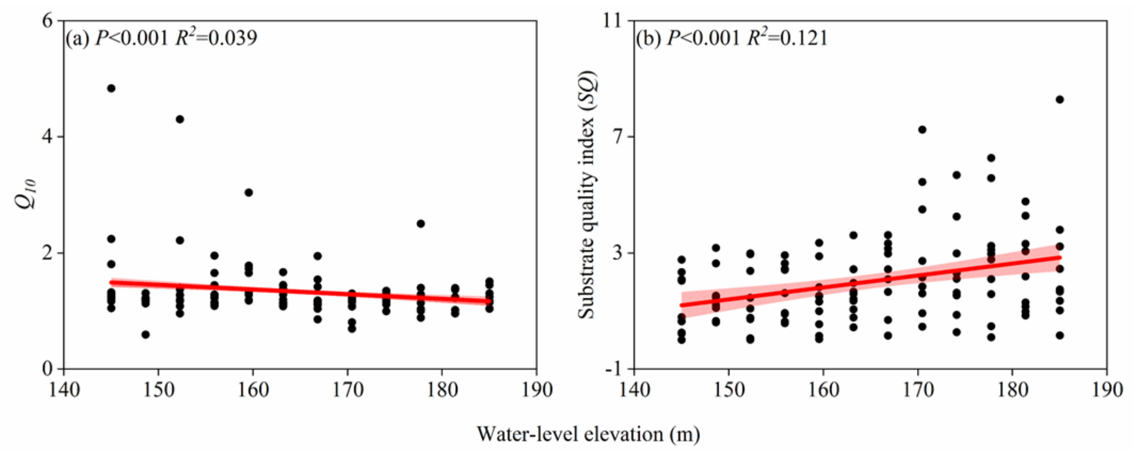

Fig. 4 Relationships between temperature sensitivity (Q_{10}) of sediment net N mineralization rate (a), substrate quality index (SQ) (b) and water-level elevations (n=132). Solid red lines represent fitted lines, and red areas below solid red lines are 95% confidence intervals.

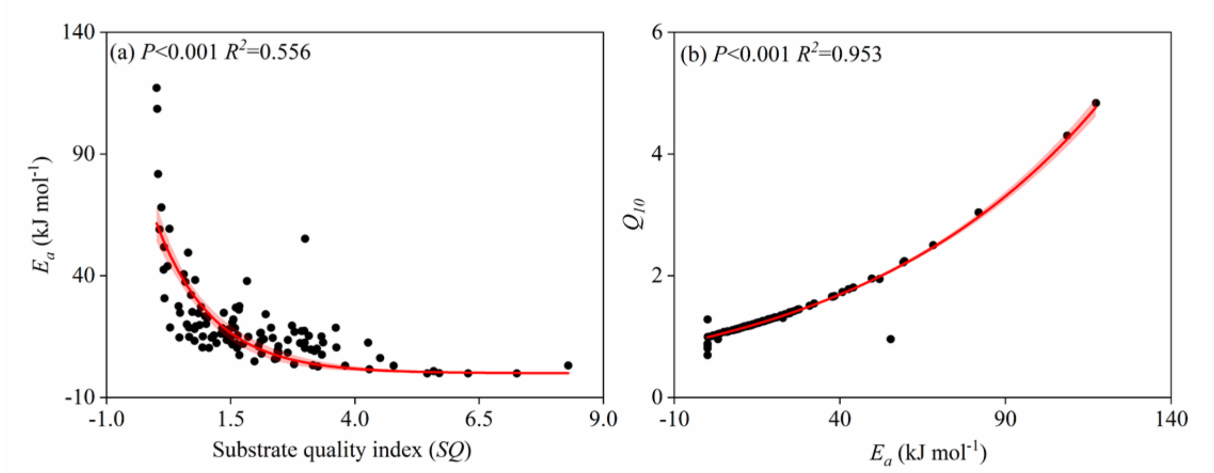

Fig. 5 Relationships between substrate quality index (SQ) (a), temperature sensitivity of sediment net N mineralization rate (Q_{10}) (b) and activation energy (E_a) (n=132). Solid red lines represent fitted lines, and red areas below solid red lines are 95% confidence intervals.

during above-mentioned sediment environments in the future. In addition, land use, topography, vegetation and revetment are also driving factors of sediment N mineralization under drying environment in riparian zone (Kikuchi et al. 2020; Yan et al. 2019; Zhang et al. 2021). Because explanations of TN and SOC by water-level elevation were just 8.4% and 14.1%, respectively, and explanation of N_{min} by TN and SOC was only 25.4% (Fig. 6), we speculate that land use, topography and vegetation may have a great influence on N_{min} in the riparian zone. So, to discover more driving factors of N_{min} in the riparian zone, *in situ* experiments considering above factors should be conducted in the future. We found that sediment TN change was another driving factor of N_{min} at water-level elevation in riparian zone, which is consistent with our hypothesis. The results mean that measures, such as removal of plant litter and prohibition of cultivation in riparian zone, should be taken to decline input of organic N during drying period, especially at low water-level elevation, for reduction of sediment N release caused by microbial mineralization during rain leaching and following flooding. Meanwhile, our results implied that water-level elevation should be considered when evaluating sediment N loss in riparian zone. In short, caused by the increase of TN with water-level elevation, N_{min} raised with water-level elevation in the riparian zone of the TGR during drying period.

4.2 Temperature sensitivity of sediment net N mineralization rate

Generally, N_{min} keeps stable after 28 days of

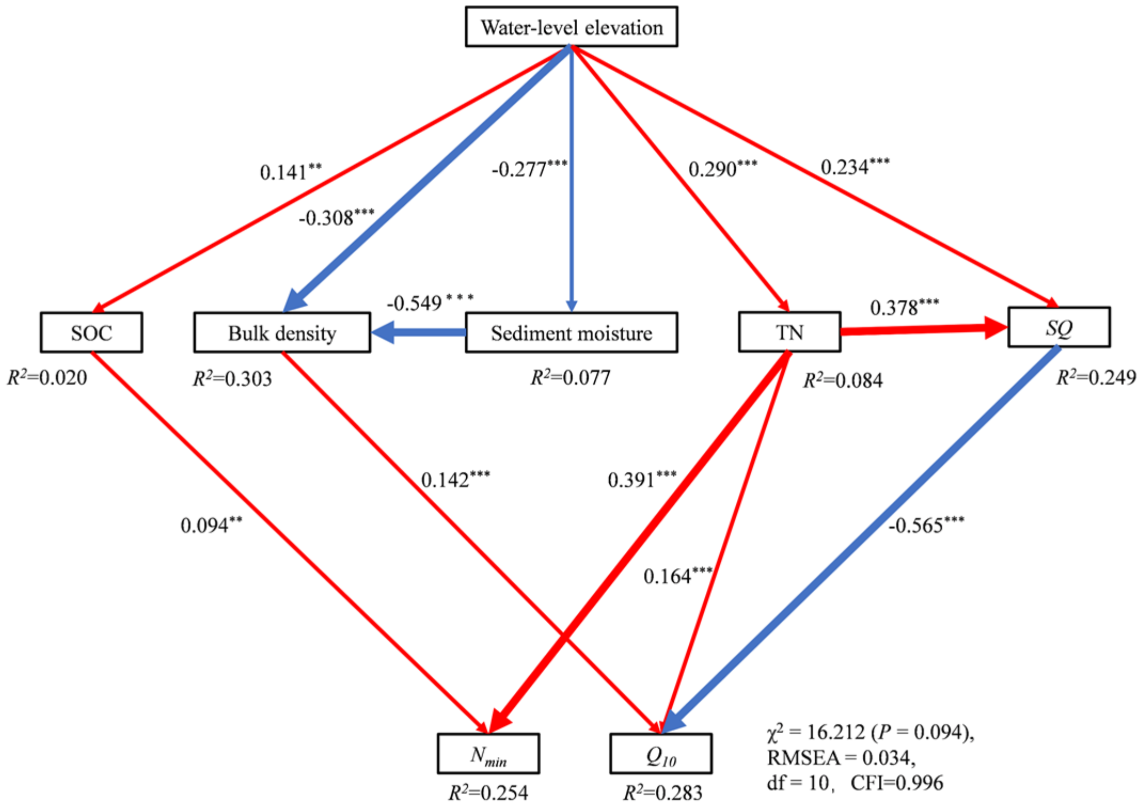

Fig. 6 The structural equation model analysis shows multivariate effects of water-level elevation change on sediment net N mineralization rate (N_{min}) and its temperature sensitivity (Q_{10}) through sediment physicochemical properties. Arrows indicate hypothesized direction of causation. Positive and negative effects are displayed by red and blue one-way arrows, respectively. Standardized path coefficients are shown next to the arrows. Solid and dashed arrows represent significant (**P<0.01; ***P<0.001) and non-significant (P>0.05) relationships, respectively. Proportions of variance explained (R^2) are shown below each response variable in the model, and results of goodness-of-fit statistics are shown alongside the model. SOC, sediment organic C; TN, total N; SQ, substrate quality index.

incubation (Jia et al. 2019), which means microbial mineralization of labile organic N has been completed, and soil N mineralization primarily comes from recalcitrant organic N (dominant component of sediment organic N). The average Q_{10} (1.34, Fig. 4) was lower than that of cropland (2.02), grassland (1.67) and forest (2.43, Liu et al. 2017). Labile organic N input from vegetation (Garssen et al. 2015; Ye et al. 2020) should be responsible for lower Q_{10} in the riparian zone compared to other ecosystems abovementioned, given the consistency of our results with the CQT hypothesis (Fig. 5). Q_{10} is unclear in riparian zone at present. The result could provide a reference for evaluation of sediment N loss from riparian zone to its surrounding water during drying period under background of global warming.

Temperature sensitivity decreased with water-level elevation (Fig. 4, P<0.05). The result indicated that sediment N mineralization was more sensitive to temperature at lower water-level elevations, raising eutrophication risk of its surrounding water. Increase of SQ with water-level elevation (P<0.05) was the main reason for this result because Q_{10} could be explained by the CQT hypothesis (Fig. 5). This interpretation was supported by the result of the structural equation model (Fig. 6) and distribution characteristic of vegetation biomass at water-level elevation in the riparian zone of the TGR as abovementioned (Garssen et al. 2015; Ye et al. 2020). Globally, Q_{10} is primarily controlled by SQ (Liu et al. 2016; Liu et al. 2017; Liu et al. 2020), which is consistent with our result. Under an environment of low temperature (-4°C–8°C), although Q_{10} is controlled by SQ in a temperate forest, Q_{10} of lower SQ is lower compared to that of higher SQ (Schütt et al. 2014), which is inconsistent with our result. Differences in sediment substrate availability could be the reason for the divergence (von Lützow and Kögel-

Knabner 2009), which needs further investigation in the future. Q_{10} increases with latitude on a global scale (Liu et al. 2017), disagreeing with our result at the vertical scale. Differences in controlling factors of SQ should be responsible for this inconsistency. Annual average temperature is major controlling factor of SQ in the above study (Liu et al. 2016; Liu et al. 2017), while it was water-level fluctuation in our study, supported by the result of the structural equation model (Fig. 6). Spatial distribution and driving factor of Q_{10} are still unclear in riparian zone at present. It should be noted that the explanations of SBD, TN and SQ by water-level elevation were just 30.3%, 8.4% and 24.9%, respectively, and the explanation of Q_{10} by SBD, TN and SQ was only 28.3% (Fig. 6). Therefore, *in situ* experiments should be conducted to explore other driving factors of Q_{10} in the future. In brief, SQ was chief driving factor resulting in decrease of Q_{10} with water-level elevation in the riparian zone.

5 Conclusion

Sediment net N mineralization rate and total N increased with water-level elevation in riparian zone of the Three Gorges Reservoir during drying period. Temperature sensitivity of sediment net N mineralization rate decreased with water-level elevation, and substrate quality showed an opposite trend. Distribution of temperature sensitivity at water-level elevation could be explained by the carbon quality temperature hypothesis. In summary, crucial driving factors of sediment net N mineralization rate and its temperature sensitivity were total N and substrate quality in terms of physicochemical properties, respectively. The results would be helpful for evaluation of sediment N release from the riparian zone to the Three Gorges Reservoir, provide scientific reference for policy-making of land management in the riparian zone and deepen our understanding of key processes of sediment net N mineralization.

Acknowledgments

This work was supported by the Program of Chongqing Science and Technology Commission (cstc2020jcyj-msxmX0095); the Science and Technology Research Program of Chongqing Municipal Education Commission (KJZD-K202001203, KJZD-K202003501); the Innovative Research Group of Universities in Chongqing (CXQT P19037).

Electronic supplementary material: Supplementary material (Appendix 1) is available in the online version of this article at https://doi.org/10.1007/s11629-022-7691-0.

References

Bao YH, Gao P, He XB (2015) The water-level fluctuation zone of Three Gorges Reservoir—A unique geomorphological unit. Earth-Sci Rev 150: 14-24. https://doi.org/10.1016/j.earscirev.2015.07.005

Chen X, Zhang S, Liu D, et al. (2019) Nutrient inputs from the leaf decay of *Cynodon dactylon* (L.) Pers in the water level fluctuation zone of a Three Gorges tributary. Sci Total Environ 688: 718-723. https://doi.org/10.1016/j.scitotenv.2019.06.357

Craine JM, Fierer N, Mclauchlan KK (2010) Widespread coupling between the rate and temperature sensitivity of organic matter decay. Nat Geosci 3(12): 854-857. https://doi.org/10.1038/ngeo1009

Davidson EA, Janssens IA (2006) Temperature sensitivity of soil carbon decomposition and feedbacks to climate change. Nature 440(7081): 165-173. https://doi.org/10.1038/nature04514

Ding J, Chen L, Zhang B, et al. (2016) Linking temperature sensitivity of soil CO_2 release to the substrate, environmental, and microbial properties across alpine ecosystems. Global Biogeochem Cy 30(9): 1310-1323. https://doi.org/10.1002/2015GB005333

Doane TA, Horwáth WR (2003) Spectrophotometric determination of nitrate with a single reagent. Anal Lett 36(12): 2713-2722. https://doi.org/10.1081/AL-120024647

Fierer N, Craine JM, Mclauchlan K, et al. (2005) Litter quality and the temperature sensitivity of decomposition. Ecology 86(2): 320-326. https://doi.org/10.1890/04-1254

Garssen AG, Baattrup‐Pedersen A, Voesenek LA, et al. (2015) Riparian plant community responses to increased flooding: A meta‐analysis. Global Change Biol 21(8): 2881-2890. https://doi.org/10.1111/gcb.12921

Gilles P, Susana B, Abbott BW, et al. (2018) Riparian corridors: A new conceptual framework for assessing nitrogen buffering across biomes. Front Env Sci-Switz 6: 47. https://doi.org/10.3389/fenvs.2018.00047

Hefting M, Clement JC, Dowrick D, et al. (2004) Water table elevation controls on soil nitrogen cycling in riparian wetlands along a European climatic gradient. Biogeochemistry 67(1): 113-134. https://doi.org/10.1023/B:BIOG.0000015320.69868.33

Jia J, Bai J, Gao H, et al. (2019) Effects of salinity and moisture on sediment net nitrogen mineralization in salt marshes of a Chinese estuary. Chemosphere 228: 174-182. https://doi.org/10.1016/j.chemosphere.2019.04.006

Kikuchi T, Kohzu A, Ouchi T, et al. (2020) Quantifying the sources and removal of nitrate in riparian and lotic environments based on land use and topographic parameters of the watershed. Ecol Indic 116: 106535. https://doi.org/10.1016/j.ecolind.2020.106535
Kirschbaum MU (1995) The temperature dependence of soil organic matter decomposition, and the effect of global warming on soil organic C storage. Soil Biol Biochem 27(6): 753-760. https://doi.org/10.1016/0038-0717(94)00242-S
Knorr W, Prentice IC, House J, et al. (2005) Long-term sensitivity of soil carbon turnover to warming. Nature 433(7023): 298-301. https://doi.org/10.1038/nature03226
Li J, Bao Y, Wei J, et al. (2019) Fractal characterization of sediment particle size distribution in the water-level fluctuation zone of the Three Gorges Reservoir, China. J Mt Sci-Engl 16(9): 2028-2038. https://doi.org/10.1007/s11629-019-5456-1
Li X, Ding C, Bu H, et al. (2020) Effects of submergence frequency on soil C: N: P ecological stoichiometry in riparian zones of Hulunbuir steppe. J Soil Sediment 20(3): 1480-1493. https://doi.org/10.1007/s11368-019-02533-x
Liu Y, He N, Wen X, et al. (2016) Patterns and regulating mechanisms of soil nitrogen mineralization and temperature sensitivity in Chinese terrestrial ecosystems. Agr Ecosyst Environ 215: 40-46. https://doi.org/10.1016/j.agee.2015.09.012
Liu Y, Wang C, He N, et al. (2017) A global synthesis of the rate and temperature sensitivity of soil nitrogen mineralization: latitudinal patterns and mechanisms. Global Change Biol 23(1): 455-464. https://doi.org/10.1111/gcb.13372
Liu Y, Wang C, Xu L, et al. (2020) Effect of grazing exclusion on the temperature sensitivity of soil net nitrogen mineralization in the Inner Mongolian grasslands. Eur J Soil Biol 97: 103171. https://doi.org/10.1016/j.ejsobi.2020.103171
Lloyd J, Taylor J (1994) On the temperature dependence of soil respiration. Funct Ecol 8: 315-323. https://doi.org/10.2307/2389824
Lupon A, Sabater F, Miñarro A, et al. (2016) Contribution of pulses of soil nitrogen mineralization and nitrification to soil nitrogen availability in three Mediterranean forests. Eur J Soil Sci 67(3): 303-313. https://doi.org/10.1111/ejss.12344
Miller KS, Daniel G (2018) Temperature sensitivity of nitrogen mineralization in agricultural soils. Biol Fert Soils 54: 853-860. https://doi.org/10.1007/s00374-018-1309-2
Nelson DW, Sommers LE (1983) Total carbon, organic carbon, and organic matter. Methods of soil analysis: Part 2 chemical and microbiological properties 9: 539-579. https://doi.org/10.2134/agronmonogr9.2.2ed.c29
Ran Y, Wu S, Zhu K, et al. (2020) Soil types differentiated their responses of aggregate stability to hydrological stresses at the riparian zones of the Three Gorges Reservoir. J Soil Sediment 20(2): 951-962. https://doi.org/10.1007/s11368-019-02410-7
Schütt M, Borken W, Spott O, et al. (2014) Temperature sensitivity of C and N mineralization in temperate forest soils at low temperatures. Soil Biol Biochem 69: 320-327. https://doi.org/10.1016/j.soilbio.2013.11.014
Shen Y, Cheng R, Xiao W, et al. (2022) Temporal dynamics of soil nutrients in the riparian zone: Effects of water fluctuations after construction of the Three Gorges Dam. Ecol Indic 139: 108865. https://doi.org/10.1016/j.ecolind.2022.108865
Song Y, Song C, Hou A, et al. (2018) Effects of temperature and root additions on soil carbon and nitrogen mineralization in a predominantly permafrost peatland. Catena 165: 381-389. https://doi.org/10.1016/j.catena.2018.02.026
Tang Q, Bao YH, He XB, et al. (2016) Flow regulation manipulates contemporary seasonal sedimentary dynamics in the reservoir fluctuation zone of the Three Gorges Reservoir, China. Sci Total Environ 548-549: 410-420. https://doi.org/10.1016/j.scitotenv.2015.12.158
Tang X, Wu M, Li R (2018) Distribution, sedimentation, and bioavailability of particulate phosphorus in the mainstream of the Three Gorges Reservoir. Water Res 140: 44-55. https://doi.org/10.1016/j.watres.2018.04.024
Verdouw H, Echteld C, Dekkers E (1978) Ammonia determination based on indophenol formation with sodium salicylate. Water Res 12(6): 399-402. https://doi.org/10.1016/0043-1354(78)90107-0
von Lützow M, Kögel-Knabner I (2009) Temperature sensitivity of soil organic matter decomposition—what do we know? Biol Fert Soils 46(1): 1-15. https://doi.org/10.1016/j.soilbio.2009.10.002
Wang T, Zhu B, Zhou M, et al. (2020) Nutrient loss from slope cropland to water in the riparian zone of the Three Gorges Reservoir: Process, pathway, and flux. Agr Ecosyst Environ 302: 107108. https://doi.org/10.1016/j.agee.2020.107108
Yan L, Xie C, Xu X, et al. (2019) Effects of revetment type on the spatial distribution of soil nitrification and denitrification in adjacent tidal urban riparian zones. Ecol Eng 132: 65-74. https://doi.org/10.1016/j.ecoleng.2019.04.005
Yang F, Wang Y, Chan Z (2015) Review of environmental conditions in the water level fluctuation zone: Perspectives on riparian vegetation engineering in the Three Gorges Reservoir. Aquat Ecosyst Health 18(2): 240-249. https://doi.org/10.1080/14634988.2015.1040332
Ye C, Butler OM, Chen C, et al. (2020) Shifts in characteristics of the plant-soil system associated with flooding and revegetation in the riparian zone of Three Gorges Reservoir, China. Geoderma 361: 114015. https://doi.org/10.1016/j.geoderma.2019.114015
Ye C, Chen C, Butler OM, et al. (2019) Spatial and temporal dynamics of nutrients in riparian soils after nine years of operation of the Three Gorges Reservoir, China. Sci Total Environ 664: 841-850. https://doi.org/10.1016/j.scitotenv.2019.02.036
Ye C, Cheng X, Liu W, et al. (2015) Revegetation impacts soil nitrogen dynamics in the water level fluctuation zone of the Three Gorges Reservoir, China. Sci Total Environ 517: 76-85. https://doi.org/10.1016/j.scitotenv.2015.02.068
Ye F, Ma MH, Wu SJ, et al. (2019) Soil properties and distribution in the riparian zone: the effects of fluctuations in water and anthropogenic disturbances. Eur J Soil Sc 70(3): 664-673. https://doi.org/10.1111/ejss.12756
Zha Y, Faeflen SW, Zhou X, et al. (2022) Redox effect on carbon and nitrogen mineralization in the drawdown zone of the Three Gorges Reservoir. Int J Environ Sci Te: 1-12. https://doi.org/10.1007/s13762-022-03950-1
Zhang M, O'Connor PJ, Zhang J, et al. (2021) Linking soil nutrient cycling and microbial community with vegetation cover in the riparian zone. Geoderma 384: 114801. https://doi.org/10.1016/j.geoderma.2020.114801
Zhao S, Zhang B, Sun X, et al. (2021) Hot spots and hot moments of nitrogen removal from hyporheic and riparian zones: A review. Sci Total Environ 762: 144168. https://doi.org/10.1016/j.scitotenv.2020.144168